



## NIH PUBLIC ACCESS

## Author Manuscript

*Nat Struct Mol Biol.* Author manuscript; available in PMC 2015 April 01.

Published in final edited form as:

*Nat Struct Mol Biol.* 2014 October ; 21(10): 871–875. doi:10.1038/nsmb.2885.

## Mechanochemical basis of protein degradation by a double-ring AAA+ machine

**Adrian O. Olivares<sup>1</sup>, Andrew R. Nager<sup>1,†</sup>, Ohad Iosefson<sup>1</sup>, Robert T. Sauer<sup>1,\*</sup>, and Tania A. Baker<sup>1,2,\*</sup>**<sup>1</sup>Department of Biology, Massachusetts Institute of Technology, Cambridge, MA, USA<sup>2</sup>Howard Hughes Medical Institute, Massachusetts Institute of Technology, Cambridge, MA, USA

### Abstract

Molecular machines containing double or single AAA+ rings power energy-dependent protein degradation and other critical cellular processes, including disaggregation and remodeling of macromolecular complexes. How the mechanical activities of double-ring and single-ring AAA+ enzymes differ is unknown. Using single-molecule optical trapping, we determine how the double-ring ClpA enzyme from *Escherichia coli* mechanically degrades proteins in complex with the ClpP peptidase. We demonstrate that ClpA unfolds some protein substrates substantially faster than the single-ring ClpX enzyme, which also degrades substrates in collaboration with ClpP. We find that ClpA is a slower polypeptide translocase and moves in physical steps that are smaller and more regular than steps taken by ClpX. These direct measurements of protein unfolding and translocation define the core mechanochemical behavior of a double-ring AAA+ machine and provide insight into the degradation of proteins that unfold via metastable intermediates.

### INTRODUCTION

AAA+ family enzymes (ATPases associated with various activities) carry out critical mechanical tasks in all cells<sup>1,2</sup>. For example, AAA+ proteases catalyze ATP-dependent protein degradation to maintain protein homeostasis and quality control in organisms from bacteria to humans<sup>3</sup>. The simplest of these proteolytic machines consist of a self-compartmentalized peptidase, in which the proteolytic active sites are sequestered within a barrel-like structure, and a homohexameric unfolding ring, in which each subunit contains a single AAA+ motor domain. In some ATP-dependent proteases, each subunit of the hexamer contains two AAA+ domains, which are organized into discrete, stacked rings in structures determined by electron microscopy and X-ray crystallography<sup>4-7</sup>. The single or double AAA+ rings of these molecular machines recognize specific degrons in target

\*Correspondence should be addressed to R.T.S. ([bobsauer@mit.edu](mailto:bobsauer@mit.edu)) or T.A.B. ([tabaker@mit.edu](mailto:tabaker@mit.edu)).

†Current address: Department of Molecular and Cellular Physiology, Stanford University School of Medicine, Stanford, CA, USA

#### AUTHOR CONTRIBUTIONS

A.O.O. performed and analyzed optical-trapping experiments, performed biochemical experiments, and constructed and purified ClpA variants. A.R.N. constructed, purified, and assembled the biotinylated, mixed-ring ClpP enzyme used for single-molecule studies. O.I. constructed and purified the multi-domain titin/GFP substrate. All authors contributed to writing the manuscript.

#### COMPETING FINANCIAL INTERESTS

The authors declare no competing financial interests.

proteins, exert an unfolding force when loops lining the axial pore grip and pull on the substrate, and then processively translocate the unfolded polypeptide into the associated peptidase for degradation<sup>3</sup> (Fig. 1a). Related single-ring and double-ring AAA+ enzymes carry out diverse protein-remodeling functions. For example, the single-ring katanin and spastin enzymes sever microtubules, whereas double-ring enzymes such as NSF, p97, and ClpB/Hsp104 disassemble SNARE complexes, extract proteins from membrane channels, and solubilize protein aggregates, respectively<sup>8-11</sup>.

ATP hydrolysis by AAA+ proteases provides the energy to power protein degradation, but it is not known how double-ring AAA+ hexamers with a total of twelve ATPase active sites differ in mechanical activity from single-ring hexamers with a total of six active sites.

*Escherichia coli* ClpAP consists of the double-ring ClpA AAA+ enzyme in complex with the ClpP peptidase<sup>4,12</sup>. The rings formed by the N-terminal and C-terminal AAA+ domains of ClpA are called D1 and D2, respectively. Elimination of ATP hydrolysis in either ring by Glu→Gln (EQ) mutations in the Walker-B ATPase motifs reduces rates of ClpAP degradation, but the D2 ring appears to be more important than D1 for unfolding and degrading more stable substrates<sup>13</sup>. The single-ring ClpX AAA+ hexamer also degrades proteins in collaboration with ClpP<sup>4</sup>. Does the double-ring structure of ClpA endow it with mechanical properties superior to ClpX? If so, does twice the number of active sites for ATP hydrolysis in ClpA double its power, speed, translocation step size, or grip on protein substrates compared to ClpX? Here, we answer these questions by using single-molecule optical trapping to determine how ClpAP mechanically unfolds and translocates multi-domain protein substrates and then comparing these activities to those determined previously for *E. coli* ClpXP<sup>14-17</sup>. We find that ClpA unfolds most protein domains substantially faster than ClpX but translocates the unfolded polypeptide more slowly, taking individual physical steps that are smaller and more regular on average. We find no evidence that ClpAP can generate more force than ClpXP, supporting a model in which a stronger grip on the substrate is responsible for faster protein unfolding by ClpA. Understanding the mechanochemical activities of these single-ring and double-ring AAA+ machines provides a foundation for understanding the diverse members of this family of protein destroying and remodeling enzymes.

## RESULTS

### Single-molecule degradation by ClpAP

We monitored single-molecule unfolding and translocation by ClpAP using a dual-laser optical trap in passive force-clamp mode<sup>14,17</sup>. We immobilized the ClpAP complex to one streptavidin-coated bead using biotinylated ClpP. One set of protein substrates consisted of a C-terminal ssrA tag (a degron for ClpAP), a 13-residue linker, four titin<sup>127</sup> domains with V13P or V15P mutations, and an N-terminal HaloTag domain (Halo), which we conjugated to a biotinylated 3500 base-pair DNA handle and attached to a second streptavidin-coated bead (Fig. 1b). Another substrate consisted of a C-terminal ssrA tag, native V13P titin<sup>127</sup>, green fluorescent protein (GFP), an unfolded titin<sup>127</sup> domain ( $\cup$ titin), GFP, and the DNA-conjugated Halo domain (Fig. 1b). Stable tethers between beads actively formed in the presence of saturating ATP. At forces from ~5-20 pN, ClpAP unfolding of individual titin<sup>127</sup>

or Halo domains resulted in an almost instantaneous increase in bead-to-bead distance (Fig. 1c) consistent with two-state, cooperative substrate unfolding<sup>14</sup>. For GFP, some ClpAP unfolding events appeared to occur in multiple sequential steps, as observed previously for ClpXP unfolding<sup>15-16</sup>. Following complete ClpAP unfolding, we observed a gradual reduction in bead-to-bead distance as the double ring of ClpA translocated the unfolded polypeptide into ClpP for degradation (Fig. 1c). Following translocation and prior to unfolding of the next domain, we observed a pre-unfolding dwell with almost no change in the bead-to-bead distance (Fig. 1c).

For the four different types of protein domains in our substrates, the distributions of pre-unfolding dwells, which provide information about the rates of enzyme-catalyzed unfolding, fit to single exponentials, although a sum of two exponentials provided a better fit for the titin<sup>I27</sup> data (Fig. 2a). Single-exponential behavior is expected if substrate unfolding follows one major pathway with a single rate-limiting kinetic transition, whereas a sum of exponentials could indicate multiple unfolding pathways. The unfolding time constants from the single-exponential fits to the titin<sup>I27</sup> domains were ~2 s ( $1.7 \pm 0.2$  s) for V13P and ~6 s ( $5.6 \pm 0.4$  s) for V15P. Unfolding time constants from double-exponential fits were  $0.30 \pm 0.08$  s (43% amplitude) and  $4.3 \pm 0.8$  s (57% amplitude) for V13P and  $0.08 \pm 0.04$  s (20% amplitude) and  $7.9 \pm 0.5$  s (80% amplitude) for V15P. Faster ClpAP unfolding of V13P is consistent with the lower thermodynamic, kinetic, and mechanical stabilities of this protein domain compared to V15P<sup>18,19</sup>. ClpXP also unfolds the V13P domain faster than V15P in single-molecule experiments, but with time constants of ~6 and ~17 s, respectively<sup>17</sup>. GFP unfolding by ClpAP proceeded with a time constant of ~3 s ( $2.7 \pm 0.2$  s) compared to ~11 s for ClpXP<sup>15,16,20</sup>. Thus, ClpAP unfolds the titin<sup>I27</sup> and GFP domains substantially faster than does ClpXP (Fig. 2b). For the Halo domain, ClpAP was only a marginally better unfoldase than ClpXP (unfolding times were  $5.5 \pm 0.2$  s for ClpAP and  $8.7 \pm 1.2$  for ClpXP; Fig. 2b). These results suggest that the unfolding activities of the double-ring ClpA enzyme and single-ring ClpX enzyme reflect differences in the physical properties of the substrate in addition to differences in enzyme mechanism and/or ring architecture. For example, Halo terminates with a helix that could be pulled apart in a step-wise manner, whereas the titin and GFP domains terminate with  $\beta$ -strands embedded in  $\beta$ -sheets, requiring simultaneous shearing of multiple hydrogen bonds to initiate unfolding.

Unfolding by AAA+ rings appears to occur when mechanical pulling, which is driven by polypeptide translocation, coincides with transient, stochastic destabilization of the substrate<sup>14</sup>. Therefore, the double-ring structure of ClpA might allow it to unfold some domains faster than ClpX because it translocates faster or takes larger steps during translocation. However, our results support neither of these possibilities. Over a range of experimental forces, ClpAP translocated unfolded polypeptides ~30% more slowly than ClpXP (Fig. 3a), and we detected no substantial changes in translocation velocity for different denatured substrate domains. During translocation, ClpXP takes physical steps ranging from 1-4 nm in length, with an average of ~2 nm<sup>14-17</sup>. By contrast, we found that ClpAP predominantly takes 1-nm translocation steps, a few 2-nm steps, and almost no 3-nm or 4-nm steps (Fig. 3b, 3c). The 2-nm steps did not occur in clusters, and we did not observe a clear pattern of 1-nm and 2-nm steps. For example, the probability of observing a 2-nm step was ~30% at the N-2, N-1, N+1, and N+2 positions relative to either a 1-nm or 2-nm

step. As translocation occurs in ~1 nm steps or multiples of this value, we conclude that the fundamental ClpAP step size, defined as the mechanical movement coupled to one ATPase cycle, is ~1 nm, which corresponds to translocation of 4-8 amino acids over the range of forces tested. This value agrees with a recent estimate of the ClpAP kinetic step size of ~5 amino acids using a single-turnover stopped-flow assay of polypeptide translocation<sup>21</sup>.

To probe the mechanochemical cycle of ClpAP, we examined the dwell times preceding each translocation step, which fit well to a sum of two exponentials, with a major population of ~90% ( $\tau = 0.4 \pm 0.01$  s) and a minor population of ~10% ( $\tau = 2.0 \pm 0.1$  s) (Fig. 3d). Dwells preceding 1-nm steps had a similar distribution to dwells preceding 2-nm steps (Fig. 3d, inset). The pre-step dwells for ClpXP were previously found to be distributed non-exponentially with an average of ~0.4-0.6 s<sup>16,17</sup>. Therefore, compared to ClpXP, the slower average translocation velocity of ClpAP results primarily from taking translocation steps of shorter length. Furthermore, most ClpAP translocation steps appear to result from a single kinetic pathway based on the stepping dwell-time kinetics described above, consistent with a rate-limiting transition likely involving ATP binding, hydrolysis, or product release in one subunit. By contrast, the majority of ClpXP steps involve the coordinated firing of multiple subunits, resulting in kinetic bursts that generate steps of ~2-4 nm<sup>16,17</sup>. The slow component of the ClpAP dwell-time distribution might represent translocation pausing, as observed with ClpXP<sup>14-17</sup>, or reflect differences between the mechanochemical cycles of the D1 and D2 ClpA AAA+ rings. For example, slower firing of subunits in D1 compared to D2 is consistent with mutagenic and biochemical studies<sup>13</sup>. However, our finding that 1-nm and 2-nm steps occur with similar kinetics (Fig. 3d inset) makes it unlikely that the D1 ring is responsible for short steps and the D2 ring for long steps or *vice versa*.

### Subunit-mixing supports non-sequential ATP hydrolysis

Our finding that ClpA takes a mixture of 1-nm and 2-nm steps with no specific sequence or pattern suggests that ATP hydrolysis has some stochastic or probabilistic character rather than being strictly sequential (see Discussion). If a defined pattern of ATP hydrolysis involving all subunits in either ClpA ring were required for mechanical activity, then elimination of ATP hydrolysis in any single subunit should prevent substrate unfolding and translocation. We initially assayed rates of ClpAP degradation of GFP-ssrA<sup>22</sup> to determine the dependence on the ATP and protein substrate concentrations (Figs. 4a, 4b). Both  $K_M$  and  $k_{deg}$  ( $V_{max}/[\text{enzyme hexamer}]$ ) for degradation of the protein substrate changed as a function of ATP concentration (Fig. 4b), and the second-order rate constant for degradation ( $k_{deg}/K_M$ ) decreased as the ATPase rate was reduced (Fig. 4c). Next, using saturating concentrations of ATP and GFP-ssrA, we assayed rates of degradation after mixing a fixed concentration of active ClpA with increasing concentrations of ClpA<sup>E286Q E565Q</sup>, a variant in which mutations in the Walker-B motifs of the D1 and D2 AAA+ domains eliminate robust ATP hydrolysis (Fig. 4d). Assuming unbiased mixing of inactive and active subunits, the results fit best to a model in which two inactive subunits in a hexamer are required to abrogate unfolding and degradation of GFP-ssrA, supporting a model in which strictly sequential ATP hydrolysis in either ring of ClpA is not required for function.

## DISCUSSION

In combination with previous single-molecule studies of ClpXP proteolysis<sup>14-17</sup>, our results indicate that ClpA and ClpX use some common and some different strategies to unfold and translocate substrate proteins into ClpP for degradation. Despite differences between the double-ring architecture of ClpA and the single-ring structure of ClpX, the size of the fundamental translocation step for both enzymes is ~1 nm. This result suggests that constraints imposed by the structures of different nucleotide states of a single AAA+ ring determine the size of a single power stroke both in single-ring and double-ring enzymes<sup>5-7,23-24</sup>. However, ClpXP takes many steps in kinetic bursts of ~1 nm, resulting in physical steps as large as 4 nm. ClpAP, by contrast, mostly takes 1-nm steps with a minority of 2-nm steps. Nevertheless, both ClpAP and ClpXP processively degrade multi-domain substrates consisting of titin, GFP, and Halo, suggesting that the ability of ClpXP to take larger physical translocation steps is not an essential factor in its ability to degrade these proteins.

To degrade GFP-ssrA, ClpXP initially extracts and translocates the ssrA-tagged  $\beta$  strand at the C-terminus, but global unfolding and degradation are unsuccessful when the rate of ATP hydrolysis is below a specific threshold value<sup>20,25</sup>. Because ClpXP does not take bursts of four highly coordinated 1-nm translocation steps at low ATP concentrations, which also fail to support GFP-ssrA degradation, Bustamante and colleagues proposed that fast 4-nm steps are required to translocate the extracted  $\beta$  strand before refolding occurs<sup>15</sup>. However, this rapid-burst model cannot account for ClpAP unfolding and translocation of GFP, as ClpAP takes essentially no 4-nm steps at saturating ATP in single-molecule experiments and yet degrades GFP-ssrA in solution and in single-molecule experiments faster than does ClpXP. Like ClpXP, ClpAP also loses the ability to degrade GFP-ssrA as its ATPase activity is reduced. We propose that both ClpXP and ClpAP fail to unfold and degrade GFP at low ATP concentrations because ATP-free subunits in the AAA+ rings of these enzymes grip the extracted  $\beta$  strand too weakly to prevent substrate release and refolding<sup>25</sup>. In support of this hypothesis, we found that  $K_M$  for ClpAP degradation of GFP-ssrA increased as the ATP concentration was reduced, as expected if substrate binding becomes weaker at lower ATP occupancies.

Why does ClpAP unfold GFP and the V13P and V15P titin domains substantially faster than ClpXP? One possibility is that the ClpA N-domain enhances substrate unfolding compared to the ClpX<sup>N</sup> variant used in single-molecule and biochemical studies. However, in the presence of ClpP, Weber-Ban and colleagues showed that ClpA missing its N-domain degrades GFP-ssrA as fast as full-length ClpA<sup>26</sup>. Because ClpX<sup>N</sup> also degrades ssrA-tagged substrates at the same rate as full-length ClpX in the presence of ClpP<sup>27</sup>, differences in the mechanochemical behavior of these two enzymes are likely to arise from differences in machine activity and not from the presence or absence of the N-domains.

There is no evidence that ClpA applies more force than ClpX, as results presented here and previously show that both machines translocate at a relatively constant speed over a wide range of applied loads and perform ~5 kT of work when taking ~1-nm steps against forces of ~20 pN<sup>14-17</sup>. We propose that the superior unfolding ability of ClpA may result because it

can grip the substrate more tightly during unfolding. The axial-pore loops in both the D1 and D2 rings of ClpA appear to interact with substrate<sup>28</sup>, roughly doubling the number of interactions that could be made in comparison with the single AAA+ ring of ClpX. This larger interaction surface for ClpA could allow tighter gripping of the substrate and increase the probability that a power stroke results in substrate unfolding rather than futile slipping of the substrate relative to the enzyme. In a tug-of-war, for example, a team that could grip the rope more tightly would have a substantial advantage over equally strong but less sure-handed opponents.

Hexameric ClpX rings with only one or two ATPase-active subunits retain the ability to unfold and translocate substrates supporting a model in which ATP hydrolysis in the ClpX AAA+ ring occurs by a mechanism that is fundamentally stochastic or probabilistic<sup>17,27</sup>. A model in which coordinated translocation bursts depend upon probabilistic ATP hydrolysis in different ClpX subunits can also explain why this enzyme takes physical steps of different sizes without a repeating pattern<sup>17</sup>. However, strictly sequential models in which pairs of subunits in a hexamer hydrolyze ATP in a cyclic pattern have been proposed for other single-ring AAA+ proteases<sup>29</sup>. Because ClpAP efficiently degrades some substrates when ATP hydrolysis in either the D1 or the D2 rings is eliminated<sup>13</sup>, it is clear that each ClpA ring can hydrolyze ATP to produce mechanical work independently of ATP hydrolysis in the other ring. Our findings that ClpA takes 1-nm and 2-nm physical translocation steps in random patterns and can tolerate at least one ATPase defective subunit in both the D1 and D2 rings without compromising GFP-ssrA degradation also suggest that strictly sequential ATP hydrolysis in either ring is unlikely to be an essential mechanistic feature. Nevertheless, whether and/or how subunits in a single ClpA ring or subunits in different rings coordinate their activities to allow unfolding of difficult substrates remains to be determined.

Bacteria and organelles contain multiple AAA+ proteases, suggesting that they play distinct biological roles. In *E. coli*, adaptor proteins ensure that ClpXP rather than ClpAP degrades most incomplete translation products bearing the tmRNA-derived ssrA tag<sup>30-33</sup>. In this regard, the faster translocation activity of ClpXP could allow faster degradation of these partial proteins, which are unlikely to be stably folded. ClpAP, by contrast, probably unfolds and degrades many endogenous native proteins faster than ClpXP, as observed for the model substrates studied here and previously<sup>30,34</sup>. In terms of the average time required for single-molecule degradation of GFP, for example, ClpAP unfolding accounts for ~20% and translocation for ~80%, but these values for ClpXP are ~60% for unfolding and ~40% for translocation. Such enzymatic “tuning” of specific substrates to specific AAA+ proteases has been previously documented<sup>34,35</sup> but is not unique to these molecular machines. For example, the myosin superfamily of actin-based molecular motors performs a wide variety of biological functions, yet shares a common mechanochemical cycle<sup>36</sup>. Specific variations in the ATPase cycles of different myosin motors provide unique adaptations allowing these enzymes to either processively move cargo, behave as anchor proteins, or work in large arrays for muscle contraction. Our results suggest that double-ring AAA+ enzymes will be able to remodel key substrates substantially faster or at a lower energetic cost than their single-ring counterparts.

## ONLINE METHODS

### Proteins

C9 variants of *E. coli* ClpA and ClpA<sup>E286Q/E565Q</sup>, a single-chain ClpX<sup>N</sup> hexamer (ClpX<sup>SC</sup>), and ssrA-tagged protein substrates were cloned, expressed, and purified as described<sup>14,17,39</sup>. Deletion of the nine C-terminal amino acids of ClpA (C9) prevents autodegradation but does not otherwise affect ClpA activity<sup>39</sup>. One of the titin<sup>127</sup> domains in the substrate containing GFP was unfolded by mutating both of its cysteines to aspartic acids<sup>40</sup>. For optical trapping, we used a tetradecameric ClpP variant consisting of one heptameric ring of wild-type *E. coli* ClpP with a C-terminal EENLYFQSH<sub>6</sub> sequence (TEV protease site underlined; ClpP-TEV-His) and one heptameric ring of the M5A ClpP variant<sup>41</sup> with a C-terminal GLNDIFEAQKIEWHH<sub>6</sub> sequence (biotin acceptor peptide sequence underlined; ClpP<sup>M5A</sup>-bAP-His). Both ClpP variants were expressed and purified on Ni-NTA resin. ClpP<sup>M5A</sup>-bAP-His was exogenously biotinylated using purified BirA enzyme, and the His<sub>6</sub>-tag of ClpP-TEV-His was removed by cleavage with TEV protease. An excess of this enzyme was mixed with ClpP<sup>M5A</sup>-bAP-His, dialyzed at 4 °C against buffer containing 150 mM ammonium sulfate to allow exchange of heptameric rings<sup>42</sup>, dialyzed at room temperature into buffer containing 150 mM KCl, and tetradecamers containing His<sub>6</sub>-tags were purified by Ni-NTA chromatography and stored at -80 °C. This procedure generates a majority of ClpP<sub>7</sub>/ClpP<sup>M5A</sup>-bAP-His<sub>7</sub> (ClpP\*) enzymes and some ClpP<sup>M5A</sup>-bAP-His<sub>7</sub>/ClpP<sup>M5A</sup>-bAP-His<sub>7</sub> enzymes, but the latter species does not bind ClpA or ClpX tightly because of the double M5A mutation.

### Single-molecule optical trapping

Complexes of ClpAP and multi-domain substrates containing an N-terminal Halo domain covalently linked to biotinylated double-stranded DNA conjugated to a HaloTag ligand (Promega, WI, USA) were tethered between two beads trapped by 1064-nm lasers in passive force-clamp mode as described<sup>14,17</sup>. Briefly, biotin-DNA-linked substrates were attached to 1- $\mu$ m streptavidin-coated polystyrene beads (Spherotech, IL, USA) that were loosely tethered to the surface of a glass cover slip via a DNA-linked glass-binding peptide aptamer<sup>43</sup>. Biotinylated ClpP was attached to a 1.26- $\mu$ m streptavidin-coated polystyrene bead in the presence of ClpA and saturating ATP (4.5 mM). Free enzymes were removed by centrifugation immediately prior to use. A weakly laser-trapped ClpAP bead was brought near a surface-tethered substrate bead. Upon substrate recognition by ClpAP, a stiff laser trap was used to rupture the aptamer-glass attachment of the substrate bead, resulting in a ClpAP-substrate complex tethered between two laser-trapped beads (Fig. 1b). As reported for ClpXP degradation of multi-domain substrates<sup>14,17</sup>, no traces contained all substrate domains presumably because ClpAP had unfolded and translocated C-terminal titin domains before measurements began. All experiments were performed at room temperature (18-20 °C), using 4.5 mM Mg<sup>2+</sup>•ATP and ATP-regeneration and oxygen-scavenging systems<sup>14</sup> in PD-T buffer (25 mM HEPES, pH 7.6, 100 mM KCl, 10 mM MgCl<sub>2</sub>, 10% glycerol, 0.1% Tween-20, and 1 mM tris(2-carboxyethyl)phosphine) supplemented with 1 mg/mL bovine serum albumin.

Data acquisition was carried out as described<sup>14</sup>. Custom MATLAB scripts were used to calculate inter-bead distances, measure the magnitude of unfolding distances, and measure the pre-unfolding dwell time between the end of one translocation event and the next unfolding event. Translocation events in each trace were fit with a linear equation to determine the average translocation speed.

### Finding steps in translocation traces

Data were collected at 3 kHz sampling frequency, decimated to 50 Hz, and individual physical steps in translocation traces were determined as described<sup>17</sup>. Briefly, to find steps in the decimated data, we used a MATLAB implementation of the chi-squared minimization method<sup>37</sup> provided by J. Kerssemakers (TU Delft). The chi-squared method requires input of the number of steps to fit within a given trace, which we estimated by taking the pair-wise distribution of decimated data. Steps smaller than 0.75 nm and backward steps or slips were combined, and the dwell time preceding a combined step was added to the dwell time of the following step.

### Biochemical assays

GFP-His<sub>6</sub>-ssrA degradation was assayed by following the loss of GFP fluorescence (excitation 470 nm; emission 540 nm). Steady-state ATP hydrolysis was monitored by following the loss of NADH absorbance at 340 nm<sup>44</sup>. Final concentrations were 147 nM ClpA hexamer or 125 nM ClpX<sup>SC</sup>, 400 nM ClpP tetradecamer, and different concentrations of GFP-His<sub>6</sub>-ssrA. Varying concentrations of Mg<sup>2+</sup>•ATP with an ATP-regeneration system (20 U/mL pyruvate kinase, 20 U/mL lactate dehydrogenase, 7.5 mM phospho(enol)pyruvate and 0.2 mM NADH) were added to give the final concentrations listed in Figs. 4a and 4b. For experiments in which active and inactive subunits were mixed, the ATP-regeneration system was present and final concentrations were 132 nM ClpA hexamer, 1.3 μM ClpP tetradecamer, 20 μM GFP-His<sub>6</sub>-ssrA, and 5 mM Mg<sup>2+</sup>•ATP. Varying concentrations of inactive ClpA were added to give the final ratios shown in Fig. 4d. Biochemical experiments were performed at ~24 °C in PD-T buffer.

### Acknowledgments

Supported by the Howard Hughes Medical Institute (HHMI) (T.A.B.) and US National Institutes of Health grant AI-16892 (R.T.S). T.A.B. is supported as an employee of HHMI. We thank T.L. Sherpa for help, S. Calmat, A. Torres-Delgado and E. Vieux (MIT) for providing proteins, and M. Aubin-Tam (TU Delft) and M. Lang (Vanderbilt University) for discussions and advice.

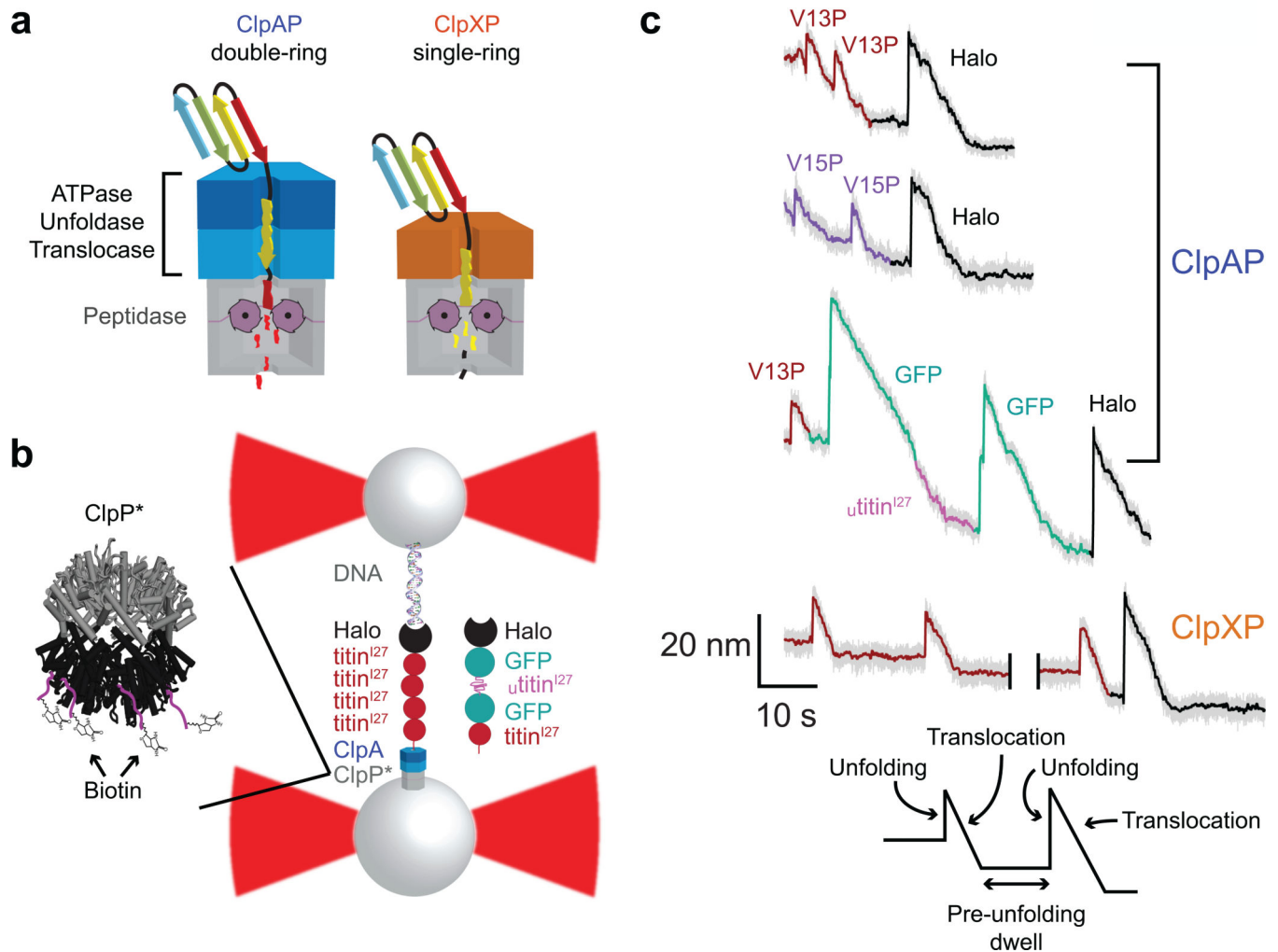
### REFERENCES

1. Neuwald AF, Aravind L, Spouge JL, Koonin EV. AAA+: A class of chaperone-like ATPases associated with assembly, operation, and disassembly of protein complexes. *Genome Res.* 1999; 9:27–43. [PubMed: 9927482]
2. Ogura T, Wilkinson AJ. AAA+ superfamily ATPases: common structure–diverse function. *Genes Cells.* 2001; 6:575–597. [PubMed: 11473577]
3. Sauer RT, Baker TA. AAA+ proteases: ATP-fueled machines of protein destruction. *Annu. Rev. Biochem.* 2011; 80:587–612. [PubMed: 21469952]

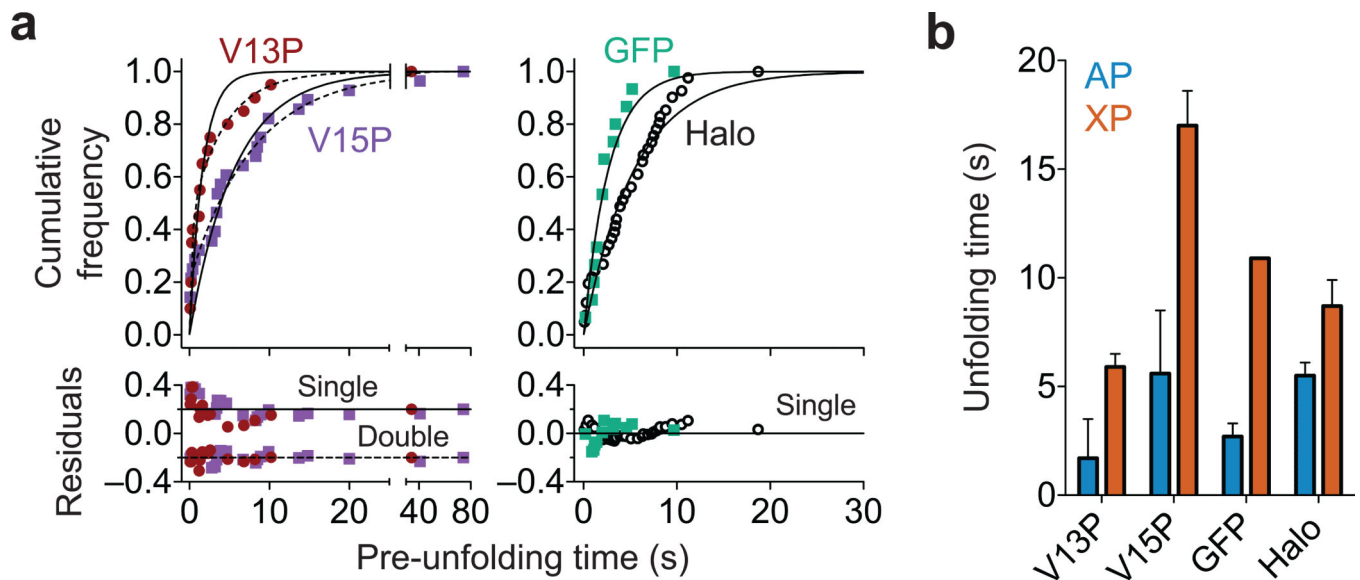


4. Grimaud R, Kessel M, Beuron F, Steven AC, Maurizi MR. Enzymatic and structural similarities between the *Escherichia coli* ATP-dependent proteases, ClpXP and ClpAP. *J. Biol. Chem.* 1998; 273:12476–12481. [PubMed: 9575205]
5. Guo F, Maurizi MR, Esser L, Xia D. Crystal structure of ClpA, an Hsp100 chaperone and regulator of ClpAP protease. *J. Biol. Chem.* 2002; 277:46743–46752. [PubMed: 12205096]
6. Wang F, et al. Structure and mechanism of the hexameric MecA-ClpC molecular machine. *Nature.* 2011; 471:331–335. [PubMed: 21368759]
7. Liu J, et al. Structural dynamics of the MecA-ClpC complex: a type II AAA+ protein unfolding machine. *J. Biol. Chem.* 2013; 288:17597–17608. [PubMed: 23595989]
8. Doyle SM, Wickner S. Hsp104 and ClpB: protein disaggregating machines. *Trends Biochem. Sci.* 2009; 34:40–48. [PubMed: 19008106]
9. Roll-Mecak A, McNally FJ. Microtubule-severing enzymes. *Curr. Opin. Cell Biol.* 2010; 22:96–103. [PubMed: 19963362]
10. Wolf DH, Stolz A. The Cdc48 machine in endoplasmic reticulum associated protein degradation. *Biochim. Biophys. Acta.* 2012; 1823:117–124. [PubMed: 21945179]
11. Zhao C, Smith EC, Whiteheart SW. Requirements for the catalytic cycle of the N-ethylmaleimide-Sensitive Factor (NSF). *Biochim. Biophys. Acta.* 2012; 1823:159–171. [PubMed: 21689688]
12. Katayama Y, et al. The two-component, ATP-dependent Clp protease of *Escherichia coli*. Purification, cloning, and mutational analysis of the ATP-binding component. *J. Biol. Chem.* 1988; 263:15226–15236. [PubMed: 3049606]
13. Kress W, Mutschler H, Weber-Ban EU. Both ATPase domains of ClpA are critical for processing of stable protein structures. *J. Biol. Chem.* 2009; 284:31441–31452. [PubMed: 19726681]
14. Aubin-Tam ME, Olivares AO, Sauer RT, Baker TA, Lang MJ. Single-molecule protein unfolding and translocation by an ATP-fueled proteolytic machine. *Cell.* 2011; 145:257–267. [PubMed: 21496645]
15. Maillard RA, et al. ClpX(P) generates mechanical force to unfold and translocate its protein substrates. *Cell.* 2011; 145:459–469. [PubMed: 21529717]
16. Sen M, et al. The ClpXP protease unfolds substrates using a constant rate of pulling but different gears. *Cell.* 2013; 155:636–646. [PubMed: 24243020]
17. Cordova JC, et al. Stochastic but highly coordinated protein unfolding and translocation by the ClpXP proteolytic machine. *Cell.* 2014; 158:647–658. [PubMed: 25083874]
18. Carrion-Vazquez M, et al. Mechanical and chemical unfolding of a single protein: a comparison. *Proc. Natl. Acad. Sci. USA.* 1999; 96:3694–3699. [PubMed: 10097099]
19. Kenniston JA, Baker TA, Fernandez JM, Sauer RT. Linkage between ATP consumption and mechanical unfolding during the protein processing reactions of an AAA+ degradation machine. *Cell.* 2003; 114:511–520. [PubMed: 12941278]
20. Martin A, Baker TA, Sauer RT. Protein unfolding by a AAA+ protease is dependent on ATP-hydrolysis rates and substrate energy landscapes. *Nat. Struct. Mol. Biol.* 2008; 15:139–145. [PubMed: 18223658]
21. Miller JM, Lin J, Li T, Lucius AL. *E. coli* ClpA catalyzed polypeptide translocation is allosterically controlled by the protease ClpP. *J. Mol. Biol.* 2013; 425:2795–2812. [PubMed: 23639359]
22. Weber-Ban EU, Reid BG, Miranker AD, Horwich AL. Global unfolding of a substrate protein by the Hsp100 chaperone ClpA. *Nature.* 1999; 401:90–93. [PubMed: 10485712]
23. Glynn SE, Martin A, Nager AR, Baker TA, Sauer RT. Structures of asymmetric ClpX hexamers reveal nucleotide-dependent motions in a AAA+ protein-unfolding machine. *Cell.* 2009; 139:744–756. [PubMed: 19914167]
24. Stinson BM, et al. Nucleotide binding and conformational switching in the hexameric ring of a AAA+ machine. *Cell.* 2013; 153:628–639. [PubMed: 23622246]
25. Nager AR, Baker TA, Sauer RT. Stepwise unfolding of a  $\beta$ -barrel protein by the AAA+ ClpXP protease. *J. Mol. Biol.* 2011; 413:4–16. [PubMed: 21821046]

26. Cranz-Mileva S, Imkamp F, Kolygo K, Maglica Z, Kress W, Weber-Ban E. The flexible attachment of the N-domains to the ClpA ring body allows their use on demand. *J. Mol. Biol.* 2008; 378:412–424. [PubMed: 18358489]
27. Martin A, Baker TA, Sauer RT. Rebuilt AAA+ motors reveal operating principles for ATP-fueled machines. *Nature.* 2005; 437:1115–1120. [PubMed: 16237435]
28. Hinnerwisch J, Fenton WA, Furtak KJ, Farr GW, Horwich AL. Loops in the central channel of ClpA chaperone mediate protein binding, unfolding, and translocation. *Cell.* 2005; 121:1029–1041. [PubMed: 15989953]
29. Smith DM, Fraga H, Reis C, Kafri G, Goldberg AL. ATP binds to proteasomal ATPases in pairs with distinct functional effects, implying an ordered reaction cycle. *Cell.* 2011; 144:526–538. [PubMed: 21335235]
30. Flynn JM, et al. Overlapping recognition determinants within the *ssrA* degradation tag allow modulation of proteolysis. *Proc. Natl. Acad. Sci. USA.* 2001; 98:10584–10589. [PubMed: 11535833]
31. Dougan DA, Reid BG, Horwich AL, Bukau B. ClpS, a substrate modulator of the ClpAP machine. *Mol. Cell.* 2002; 9:673–683. [PubMed: 11931773]
32. Farrell CM, Grossman AD, Sauer RT. Cytoplasmic degradation of *ssrA*-tagged proteins. *Mol. Microbiol.* 2005; 57:1750–1761. [PubMed: 16135238]
33. Moore SD, Sauer RT. The tmRNA system for translational surveillance and ribosome rescue. *Annu. Rev. Biochem.* 2007; 76:101–124. [PubMed: 17291191]
34. Koodathingal P, et al. ATP-dependent proteases differ substantially in their ability to unfold globular proteins. *J. Biol. Chem.* 2009; 284:18674–18684. [PubMed: 19383601]
35. Gur E, Vishkautzan M, Sauer RT. Protein unfolding and degradation by the AAA+ Lon protease. *Protein Sci.* 2012; 21:268–278. [PubMed: 22162032]
36. De La Cruz EM, Ostap EM. Relating biochemistry and function in the myosin superfamily. *Curr. Opin. Cell. Biol.* 2004; 16:61–67. [PubMed: 15037306]
37. Kerssemakers JW, et al. Assembly dynamics of microtubules at molecular resolution. *Nature.* 2006; 442:709–712. [PubMed: 16799566]
38. Werbeck ND, Schlee S, Reinstein J. Coupling and dynamics of subunits in the hexameric AAA+ chaperone ClpB. *J. Mol. Biol.* 2008; 378:178–190. [PubMed: 18343405]
39. Maglica Z, Striebel F, Weber-Ban E. An intrinsic degradation tag on the ClpA C-terminus regulates the balance of ClpAP complexes with different substrate specificity. *J. Mol. Biol.* 2008; 384:503–511. [PubMed: 18835567]
40. Gur E, Sauer RT. Recognition of misfolded proteins by Lon, a AAA+ protease. *Genes Dev.* 2008; 22:2267–2277. [PubMed: 18708584]
41. Bewley MC, Graziano V, Griffin K, Flanagan JM. The asymmetry in the mature amino-terminus of ClpP facilitates a local symmetry match in ClpAP and ClpXP complexes. *J. Struct. Biol.* 2006; 153:113–128. [PubMed: 16406682]
42. Maurizi MR, Singh SK, Thompson MW, Kessel M, Ginsburg A. Molecular properties of ClpAP protease of *Escherichia coli*: ATP-dependent association of ClpA and ClpP. *Biochemistry.* 1998; 37:7778–7786. [PubMed: 9601038]
43. Aubin-Tam ME, et al. Adhesion through single peptide aptamers. *J. Phys. Chem. A.* 2011; 115:3657–3664. [PubMed: 20795685]
44. Kim YI, Burton RE, Burton BM, Sauer RT, Baker TA. Dynamics of substrate denaturation and translocation by the ClpXP degradation machine. *Mol. Cell.* 2000; 5:639–648. [PubMed: 10882100]

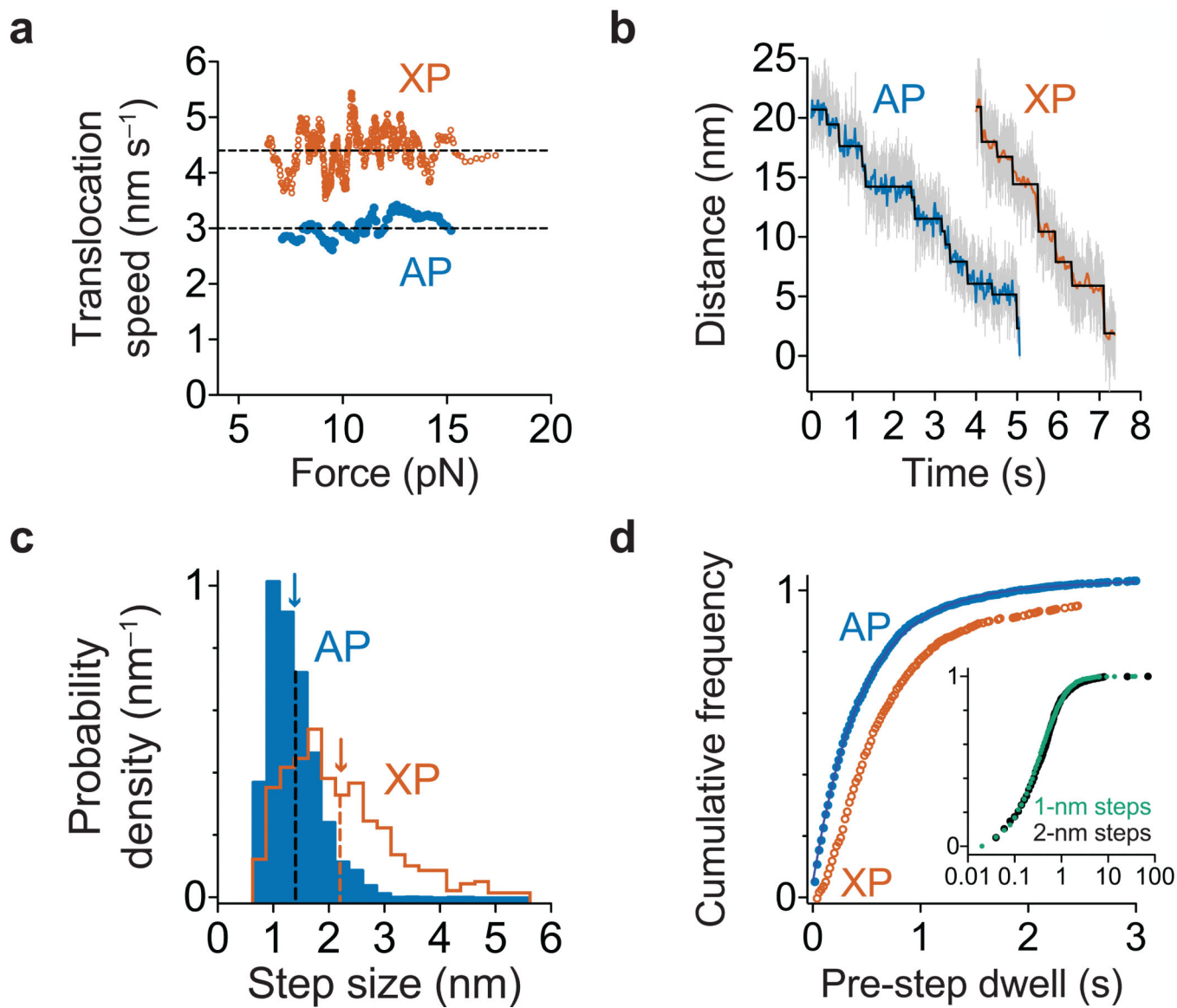


**Figure 1.** Single-molecule protein degradation by ClpAP. **(a)** Cartoon representation of ClpAP and ClpXP, which consist of the ClpP peptidase and the double-ring ClpA or single-ring ClpX unfoldase/translocase, respectively. **(b)** Experimental setup used in single-molecule measurements. An enzyme-multi-domain protein substrate complex is tethered between two laser-trapped streptavidin-coated beads. The use of a biotinylated variant of ClpP allows for the assembly and attachment of the ClpAP complex to one of the beads. **(c)** Representative traces of single-molecule protein degradation by ClpAP and ClpXP. Changes in bead-to-bead distance occur as ClpAP unfolds (sharp increases) and translocates (slower decreases) individual domains of the substrate in the presence of saturating ATP. Traces include the degradation of Halo-(V13P titin<sup>I27</sup>)<sub>4</sub>-ssrA, Halo-(V13P titin<sup>I27</sup>)<sub>4</sub>-ssrA, and Halo-GFP-( $\cup$ titin<sup>I27</sup>-GFP-(V13P titin<sup>I27</sup>))-ssrA substrates (decimated to 500 Hz in gray or 10 Hz in color). Unfolding/translocation traces are colored dark red, purple, pink, green or black for V13P titin<sup>I27</sup>, V15P titin<sup>I27</sup>,  $\cup$ titin<sup>I27</sup>, GFP, and Halo, respectively. A 40-s gap was introduced in the ClpXP trace for presentation. ClpXP data are from ref. 17 and shown here for comparison.



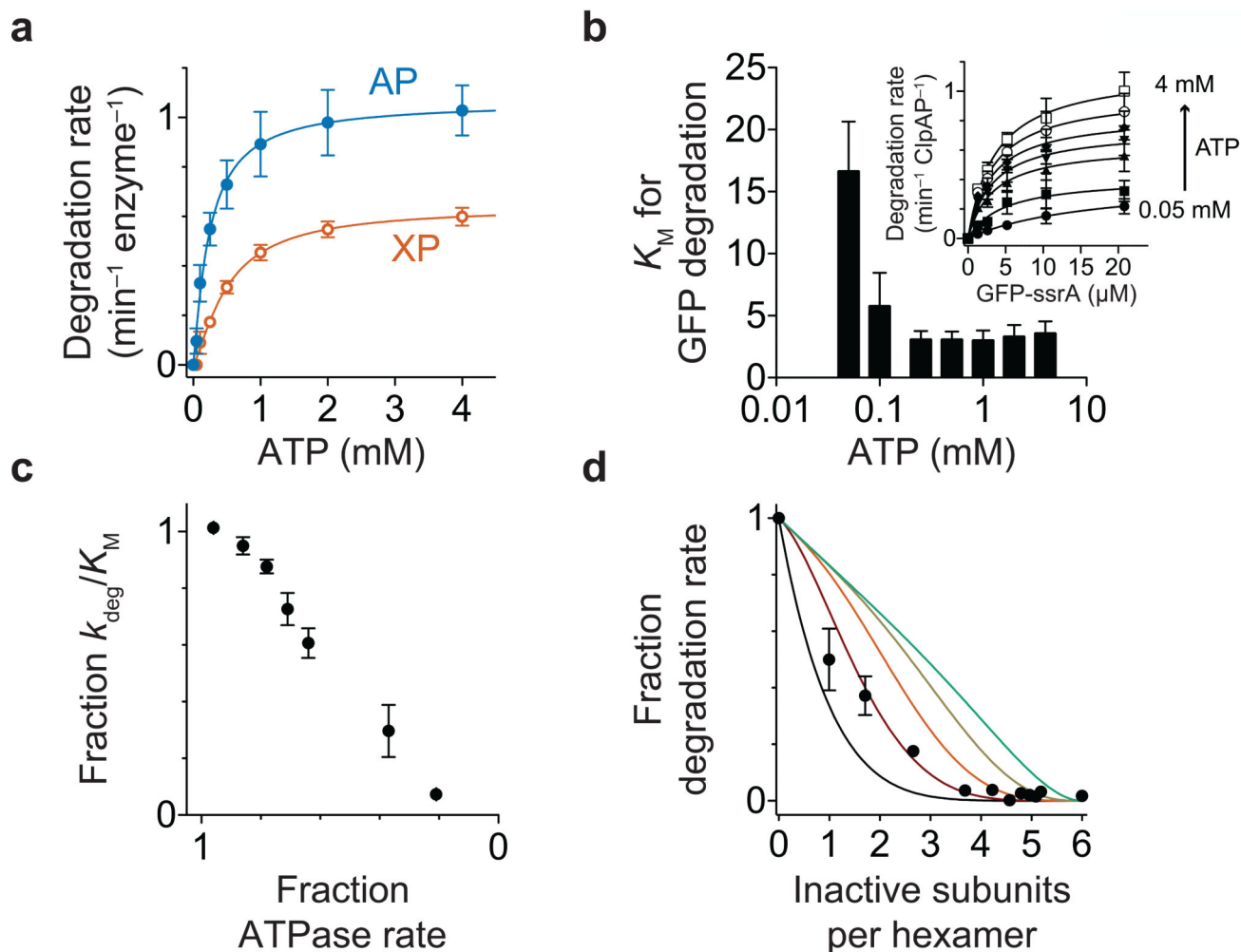
**Figure 2.**

ClpAP unfolding of different protein domains. **(a)** Distributions of ClpAP pre-unfolding dwell times depend on domain identity and stability. Single-exponential fits to the distributions are shown as solid lines. As observed with ClpXP unfolding of V13P and V15P<sup>17</sup>, the distributions of V13P and V15P domain unfolding by ClpAP were better fit to double exponentials (dashed lines). Residuals to the fits are shown. **(b)** Unfolding times from single exponential fits of pre-unfolding dwell distributions show that ClpAP unfolds titin domains ~3-4-fold faster than ClpXP but unfolds Halo with similar kinetics. Values are time constants  $\pm$  s.e.m. (ClpAP: V13P  $n = 20$ , V15P  $n = 28$ , GFP  $n = 15$ , Halo  $n = 20$  unfolding events; ClpXP: V13P  $n = 278$ , V15P  $n = 127$ , Halo  $n = 73$  unfolding events). ClpXP titin and Halo data are from ref. 17 and are shown for comparison. The ClpXP GFP unfolding time is the average of four values from refs. 15, 16 and 20.



**Figure 3.** Polypeptide translocation. **(a)** Translocation speeds for ClpAP and ClpXP. Moving-window averages of 30 consecutive titin values from combined V13P and V15P domains ranked by increasing force are shown. ClpXP titin data are from ref. 17. **(b)** Representative traces of polypeptide translocation on unfolded titin for ClpAP ( $n = 127$  domain translocation events) and ClpXP (from ref. 17) at  $\sim 13$  pN. Raw data were decimated to 1 kHz (gray) or 50 Hz (blue for ClpAP and orange for ClpXP). Chi-square fits<sup>37</sup> to the 50 Hz data are shown in black. **(c)** Blue bars show the distribution of ClpAP physical step sizes during translocation of titin and GFP domains ( $n = 2642$  steps) with a mean of  $1.4 \pm 0.5$  nm (blue arrow). The ClpXP step-size distribution (previously published in ref. 17) is shown in orange for comparison. **(d)** Distributions of dwell times preceding a step during titin and GFP translocation are shown for ClpAP (blue;  $n = 2585$  dwell times) and ClpXP (orange; data

from ref. 17). For ClpAP, the solid line is a fit to a sum of exponentials. Inset: Dwells preceding ClpAP steps of 1 and 2 nm in size are shown.

**Figure 4.**

Degradation of GFP-ssrA. (a) ATP-dependence of degradation of GFP-ssrA (20  $\mu\text{M}$ ) by ClpAP and ClpXP. Solid lines are fits to the Hill form of the Michaelis-Menten equation with maximal degradation rates of  $1.3 \pm 0.04 \text{ min}^{-1} \text{ ClpAP}^{-1}$  and  $0.7 \pm 0.05 \text{ min}^{-1} \text{ ClpXP}^{-1}$ . (b) The  $K_M$  for ClpAP degradation of the GFP-ssrA substrate increased with decreasing ATP concentration. Inset: Dependence of ClpAP degradation rates on GFP-ssrA concentration at different ATP concentrations. Solid lines are fits to the Michaelis-Menten equation:  $\text{rate} = k_{\text{deg}} \cdot [\text{GFP-ssrA}] / (K_M + [\text{GFP-ssrA}])$ , where  $k_{\text{deg}} = V_{\text{max}} / [\text{enzyme hexamer}]$ . (c)  $k_{\text{deg}}/K_M$  for ClpAP degradation of GFP-ssrA decreased as ATPase activity decreased. (d) Incorporation of ATPase inactive ClpA subunits affects GFP-ssrA degradation by wild-type ClpAP. Solid lines show simulations of degradation activity if different numbers of inactive subunits abrogate wild-type ClpAP degradation activity<sup>38</sup>. In a strictly sequential model, inactivation of one subunit would completely halt enzyme activity (black line). Error bars for all panels are s.e.m. (n = 3 independent experiments).